energy&fuels

Article

pubs.acs.org/EF

Effect of the Presence of Hydrogen Sulfide on the Formation of Light Gases, Soot, and PAH during the Pyrolysis of Ethylene

Fausto Viteri,[†,‡] Adrián Sánchez,[†] Ángela Millera,[†] Rafael Bilbao,[†] and María U. Alzueta*[,†]

[†]Aragón Institute of Engineering Research (I3A), Department of Chemical and Environmental Engineering, University of Zaragoza, Río Ebro Campus, 50018 Zaragoza, Spain

[‡]Facultad de Ciencias de la Ingeniería, Universidad Tecnológica Equinoccial, Quito EC170147, Ecuador

ABSTRACT: The formation of light gases, soot, and 16 polycyclic aromatic hydrocarbons (EPA-PAH), classified as priority pollutants by the United States Environmental Protection Agency (USEPA), has been studied during the pyrolysis of mixtures of ethylene with hydrogen sulfide (H_2S) in a tubular flow reactor setup. The study was made using a constant concentration of ethylene and different inlet concentrations of H_2S, in a temperature range from 1075 to 1475 K. The light gases produced were quantified by a chromatographic method. The soot amount formed was also quantified at the outlet of the reactor. The speciation of the individual EPA-PAH compounds was made by a combination of Soxhlet extraction, extract concentration by a rotary evaporator, and gas chromatography coupled to mass spectrometry. The present study shows that, under pyrolysis conditions, there is an effective interaction between H_2S and hydrocarbons, forming significant amounts of CS_2 and bonding sulfur to soot. The presence of H_2S in the pyrolysis of ethylene contributes to slightly decrease the formation of soot and EPA-PAH, which indicates a positive effect of the sulfur compound under pyrolysis conditions.

1. INTRODUCTION

The exploitation of sour gases presents a clear interest given the high amount of proved reserves of these gases, around 15% of the total natural gas.[1,2] However, sour gases contain significant fractions of hydrogen sulfide (around 30% by volume) and carbon dioxide, which implies a corrosion risk and a low heating value, respectively. Cleaning procedures are used to purify the sour gases, involving an additional cost. Recently, Bongartz and Ghoniem[3] proposed the oxy-fuel combustion as a new way to use the sour gas as a fuel, combining it with an enhanced oil recovery.

On the other hand, processes such as the Claus one use sour gases to recover elemental sulfur.[4] Under fuel rich conditions of the Claus process, some contaminants in its feed are capable to continue different chemical pathways originating polycyclic aromatic hydrocarbons (PAH) and carbonaceous particles (soot) that may clog the catalyst pores and produce its deactivation.[5]

PAH are important because of their relation to soot formation. The hydrogen abstraction/acetylene addition (HACA route) is the most recognized theory that explains the role of PAH during soot formation[6] and involves consecutive stages of hydrogen abstraction and acetylene addition, promoting PAH molecular growth and the subsequent soot formation. The PAH study is also important because, during the combustion process, they may be directly emitted to the atmosphere as a part of the exhaust gases, or they can remain adsorbed on the soot surface, producing carcinogenic and mutagenic effects.[7]

Little is known about the behavior of the sour gases in different combustion conditions. Mohammed et al.[5] developed a mechanism for PAH formation (up to coronene) applied to the Claus process. Selim et al.[8] and Chin et al.[9] studied the oxidation of methane and hydrogen sulfide, finding a high presence of CO and CS_2 under fuel rich conditions. Glarborg and Marshall[10] and Glarborg et al.[11] studied the dry oxidation of COS and CS_2, addressing mainly fuel lean conditions. Abián et al.[12] studied the conversion of CS_2 and COS under different combustion conditions and developed a kinetic mechanism for CS_2 oxidation. Recently, Bongartz and Ghoniem[3] developed a mechanism for oxy-fuel combustion of mixtures of hydrogen sulfide and methane and examined the influence of the sour gas composition on ignition delay and burning velocity.[13]

In addition, the interaction between sulfur compounds, as sulfur dioxide, and carbon in combustion processes has been analyzed in previous studies.[14−18] Abián et al.[16] and Viteri et al.[18] evaluated the effect of SO_2 on the formation of soot and PAH, respectively, and the results suggested a direct influence of SO_2 on their formation. Streibel et al.[17] studied the influence of the addition of sulfur, either as ammonium sulfate or as elemental sulfur, on PAH concentration during biomass combustion, and found a decrease in the PAH emissions and other unburned compounds.

In this context, the present study aims to evaluate the light gases, soot, and PAH formed from the pyrolysis of different mixtures of ethylene−hydrogen sulfide with different H_2S inlet concentrations and reaction temperatures. Ethylene was used because it is considered one of the main soot precursors in combustion processes. The study of PAH is focused on 16 priority PAH that are considered by the United States Environmental Protection Agency (USEPA) as priority pollutants, due to their carcinogenic and mutagenic properties.[19] They are called EPA-PAH in the present work.

Received: May 26, 2016
Revised: August 30, 2016

DOI: 10.1021/acs.energyfuels.6b01271
Energy Fuels XXXX, XXX, XXX−XXX

2. EXPERIMENTAL METHODOLOGY

The experiments were carried out under well controlled laboratory conditions. The reactant gas contains a constant inlet concentration of 3% ethylene, and different inlet concentrations of H_2S: 0, 0.3, 0.5 and 1%, all by volume. Nitrogen was used as diluent. The EPA-PAH analyzed are shown in Table 1.

Table 1. Abbreviations, Molecular Weights, and Empirical Formulas of Each EPA-PAH

EPA-PAH	EPA-PAH abbreviation	molecular mass (g/mol)	empirical formula
naphthalene	NAPH	128	$C_{10}H_8$
acenaphthylene	ACNY	152	$C_{12}H_8$
acenaphthene	ACN	154	$C_{12}H_{10}$
fluorene	FLUO	166	$C_{13}H_{10}$
phenanthrene	PHEN	178	$C_{14}H_{10}$
anthracene	ANTH	178	$C_{14}H_{10}$
fluoranthene	FANTH	202	$C_{16}H_{10}$
pyrene	PYR	202	$C_{16}H_{10}$
benzo(a)anthracene	B(a)A	228	$C_{18}H_{12}$
chrysene	CHR	228	$C_{18}H_{12}$
benzo(b)fluoranthene	B(b)F	252	$C_{20}H_{12}$
benzo(k)fluoranthene	B(k)F	252	$C_{20}H_{12}$
benzo(a)pyrene	B(a)P	252	$C_{20}H_{12}$
indeno(1,2,3-cd)pyrene	I(123-cd)P	276	$C_{22}H_{12}$
dibenz(a,h)anthracene	DB(ah)A	278	$C_{22}H_{14}$
benzo(g,h,i)perylene	B(ghi)P	276	$C_{22}H_{12}$

The experimental facility used in the present work is described in detail elsewhere,[20] and only a brief description is given here.

The installation consists of different systems such as gas feeding, reaction, collecting of soot and EPA-PAH, and gas analysis. Reactants, from pressurized gas cylinders, are fed by mass flow controllers to the reaction system. The reaction system consists of a vertical quartz flow reactor, with 45 mm inside diameter and 800 mm in length. The reactor is placed inside an electric furnace. The reactor inlet and outlet are cooled by compressed air, through quartz jackets, allowing a quasi-isothermal zone of 160 mm inside the reactor. The temperatures studied are in the range of 1075−1475 K. The total flow rate is 1000 mL(STP)/min, which results in a temperature-dependent gas residence time in the reaction zone between 2.83 and 3.88 s. The gas residence time, t_r, can be calculated as a function of the reaction volume, total gas flow rate, and the reaction temperature in each experiment, t_r (s) = 4168/T (K). Each experiment lasts 3 h, which is enough time to get the sufficient amount of soot for further analysis.

The collection system is placed at the reactor outlet and collects the soot and EPA-PAH formed during each experiment. The soot collection system consists of a quartz fiber filter with a pore diameter lower than 1 μm. The EPA-PAH collection system, for the gas phase, consists of an XAD-2 resin packaged in a thin tube of 300 mm in length and 10 mm in external diameter. This resin is distributed in two parts within this tube. The first part, with 3 g of resin, was used for collecting the majority of EPA-PAH, and the second part, with 2 g of resin, is used as a blank to ensure that all EPA-PAH were previously adsorbed on the first part. Regarding their molecular weight, the heaviest EPA-PAH could be found mainly adsorbed on the soot and on the reactor walls, and the lightest ones could be adsorbed on the resin.[21] The EPA-PAH fraction stuck on the reactor walls is recovered by washing the reactor with 150 mL of dichloromethane, once each experiment is finished.

The gas analysis system is connected after the soot and PAH collection system, and the gas flow passes through a gas chromatograph (GC), equipped with a thermal conductivity detector (TCD) and HP Plot MoleSieve and HP Plot Q columns, and a flame ionization detector (FID) with an HP-Pona column. This GC is calibrated to quantify H_2, CH_4, C_2H_2, C_2H_4, C_2H_6, C_3H_4 (propadiene), C_3H_6, C_3H_8, 1,3-butadiene, i-C_4H_{10}, n-C_4H_{10}, C_6H_6, C_7H_8, C_8H_{10}, and CS_2. A microchromatograph is used to measure H_2S, and it is equipped with micro-TCD detectors and four independent columns: OV-1, Plot-U, Stabilwax, and Molsieve. The measurement uncertainties for the chromatographs are estimated as ±5%.

The method used to analyze EPA-PAH has been used successfully in previous studies[20−22] and is detailed in the work of Sánchez et al.[23] A short summary is shown here. The method consists of EPA-PAH extraction by a Soxhlet system, with dichloromethane as solvent, and after the samples obtained are reduced to an adequate volume by using a rotary evaporator. Finally, the samples are immediately analyzed by a gas chromatograph coupled to a mass spectrometer (GC/MS), equipped with a 60 m long DB-17Ms fused silica capillary column (0.25 mm ID, 0.25 mm film thickness). Internal standards are used for the quantification procedure. The samples were injected (1 μL) in splitless mode. The quantification method has demonstrated recoveries higher than 80%, which agrees with the EPA criterion of acceptable recovery between 60% and 120%.[24]

Analysis to determine the percentage of elemental sulfur present in the soot samples was made.

Repeatability experiments have shown a variation lower than 0.5% of soot weight between experiments.

The experiments performed are shown in the Table 2, which also includes an experiment of C_2H_4 pyrolysis in the absence of H_2S made in a previous work.[18]

Table 2. Experimental Conditions Considered in the Present Work

set	C_2H_4 (%)	H_2S (%)	T (K)	residence time, t_r (s)	source
1	3	0.3	1475	2.83	present work
2	3	0.5	1475	2.83	present work
3	3	1	1075	3.88	present work
4	3	1	1175	3.55	present work
5	3	1	1275	3.27	present work
6	3	1	1375	3.04	present work
7	3	1	1475	2.83	present work
8	3		1475	2.83	ref 18

3. RESULTS AND DISCUSSION

The influence of the presence of H_2S on the production of light gases, soot, and EPA-PAH was evaluated in the pyrolysis of C_2H_4−H_2S mixtures, varying the H_2S inlet concentration and the reaction temperature.

For a reaction temperature of 1475 K, Figure 1a,b shows the main products formed as a function of the inlet H_2S concentration: soot, EPA-PAH, and benzene in Figure 1a, and H_2, C_2H_2, and CH_4 in Figure 1b. The conversion of C_2H_4 and H_2S and concentration of CS_2 are shown in Figure 1c.

Soot is found to decrease slightly as the H_2S concentration is increased, i.e., barely 5%. The impact of H_2S is found to be more important for the EPA-PAH quantified with a decrease of 25% with the addition of 1% H_2S with respect to the pyrolysis of pure ethylene (0% H_2S).

The presence of different amounts of H_2S produces different concentrations of the gases detected during the pyrolysis of the C_2H_4−H_2S mixtures. Whereas the presence of H_2S does not affect considerably the benzene amounts, the concentrations of H_2, CH_4, C_2H_2, and CS_2 are significantly modified.

H_2 is the major gas compound and is found in high concentration. It increases as the H_2S inlet concentration increases, coinciding with the decrease in the formation of soot observed. The increase of H_2 can be explained because of the

DOI: 10.1021/acs.energyfuels.6b01271
Energy Fuels XXXX, XXX, XXX−XXX

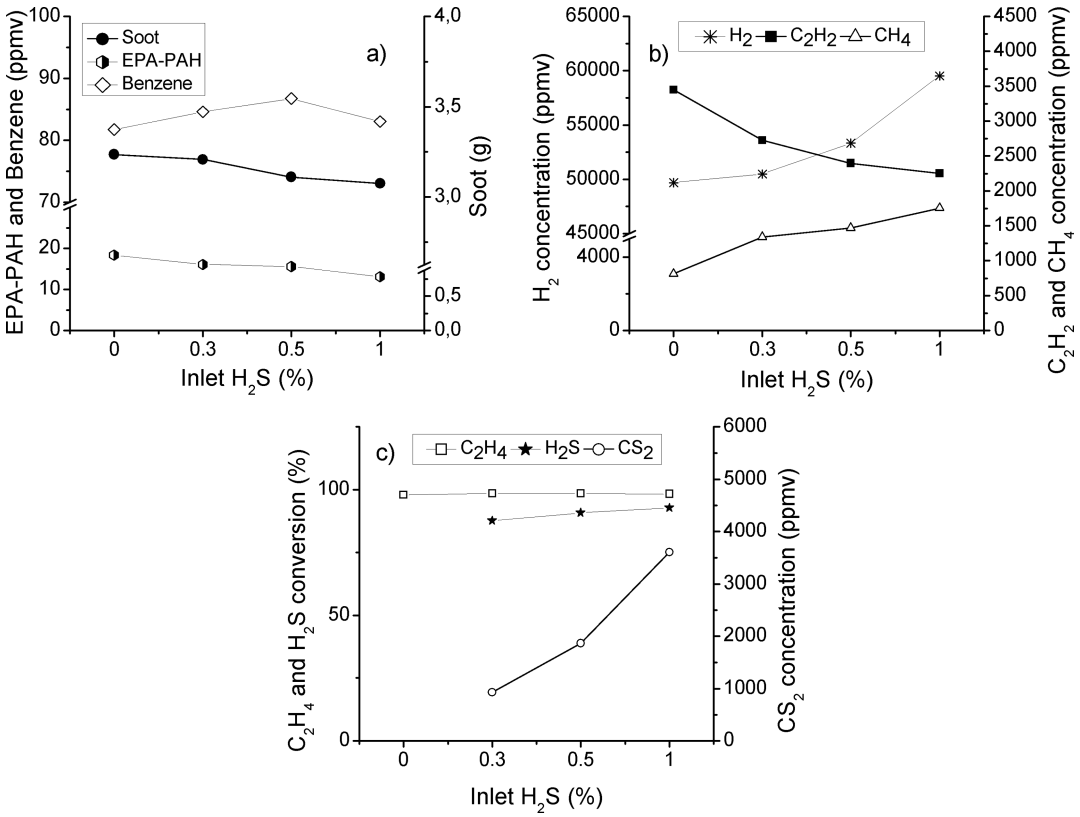

Figure 1. Products formed from the pyrolysis of C_2H_4−H_2S mixtures as a function of the inlet H_2S concentration at 1475 K. (a) Benzene, EPA-PAH, and soot amounts. (b) H_2, C_2H_2, and CH_4 concentrations. (c) C_2H_4 and H_2S conversion and CS_2 concentration. Sets 1−3, 8 in Table 2.

increment of the hydrogen amount at the inlet when the H_2S concentration is raised.

It is remarkable that, in the presence of H_2S, a significant fraction of the reactant carbon appears as reaction products in the form of CH_4 and CS_2, which do not participate in the HACA route and thus contribute to carbon removal from the typical pathways leading to PAH and soot.[16] Both, CH_4 and in particular CS_2 concentrations are increased when the inlet concentration of H_2S is increased. Other C_2−C_8 hydrocarbon species were detected in very small amounts at 1475 K, near to the measurement uncertainties, showing no significant contribution.

Among the sulfur products at the exit of the reactor such as CS_2, unreacted H_2S, and sulfur bonded to soot, the CS_2 concentrations obtained indicate that a high fraction of the sulfur in H_2S interacts with hydrocarbons (C_2H_4 and derivatives) to produce C−S bonds. For the inlet concentration of 1% H_2S, 3611 ppm of CS_2 is formed, which implies 7222 ppm of S, i.e., approximately 72% of the S in inlet H_2S that produces CS_2. This fact has already been observed in the Claus process[8] where the CH_4 present in the feeding interacts with sulfur compounds and produces CS_2 through the following reactions:[8]

$$CH_4 + 2S_2 \rightleftarrows CS_2 + 2H_2S \quad \text{(R1)}$$

$$CH_4 + 2S \rightleftarrows CS_2 + 2H_2 \quad \text{(R2)}$$

$$CH_4 + 2H_2S \rightleftarrows CS_2 + 4H_2 \quad \text{(R3)}$$

The reactions of CH_4 with sulfur compounds are very rapid and exhibit a complete conversion of the limiting reactant within the Claus furnace in less than 100 ms;[25] therefore, it is not strange to find significant amounts of CS_2 under the conditions of the present work where the lowest residence time is 2.83 s.

Elemental analysis of the soot samples, in order to determine the proportion of sulfur bound to it, shows that the content of S in the soot structure ranges 3−4% in weight. The results found in the present work are in agreement with those obtained in other works in which soot formation in the presence of SO_2 was analyzed, where S bound to soot was around 3% in weight under similar experimental conditions.[16,18] In those previous studies, using a 3% C_2H_4 mixed with 1% SO_2 at 1475 K, the influence of SO_2 on the formation of soot and EPA-PAH was analyzed, finding a high response to reduce both products, including a soot reduction percentage of 20.1%[16] and EPA-PAH reduction of 58.7%.[18] Besides the presence of sulfur in the reaction, which formed significant amounts of CS_2 (similar to those found in the present work), the decrease of soot and EPA-PAH also could be due to oxidation reactions that could have increased the removal of carbon from the pathways that lead to the formation of EPA-PAH and soot, forming products such as CO, CO_2, and COS.

The EPA-PAH are distributed in the outlet gas, adsorbed on soot, and stuck on the reactor walls. For the experiments in the presence of H_2S at the highest temperature tested (1475 K), the average distribution of the EPA-PAH was 69.7% adsorbed on soot, 28.9% in the outlet gases, and 1.3% stuck on the reactor walls. A similar trend, for the EPA-PAH distribution, was seen by Sánchez et al.,[26] who studied the pyrolysis of acetylene and ethylene, indicating that the addition of H_2S does not affect appreciably this distribution of the EPA-PAH in the different phases analyzed.

DOI: 10.1021/acs.energyfuels.6b01271
Energy Fuels XXXX, XXX, XXX−XXX

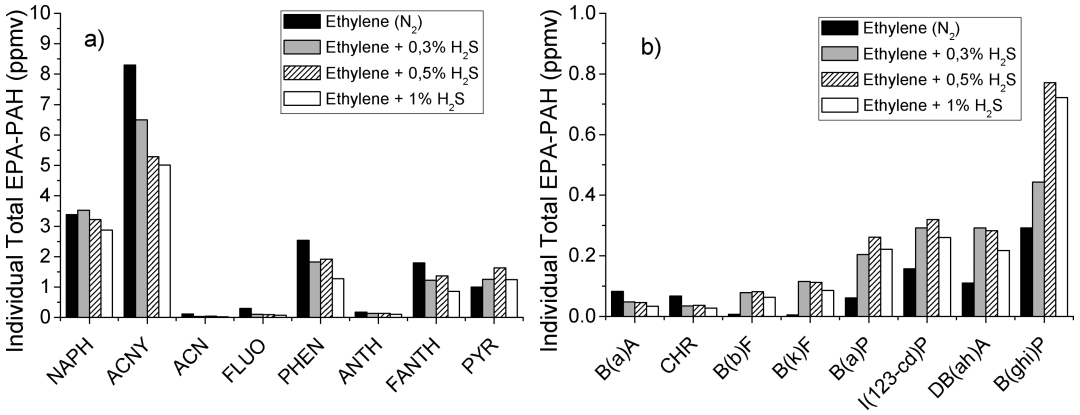

Figure 2. Individual total EPA-PAH concentration as a function of inlet H_2S concentration at 1475 K. (a) EPA-PAH (C_{10}−C_{16}). (b) EPA-PAH (C_{18}−C_{22}). Sets 1−3, 8 in Table 2.

Figure 2 shows the individual total EPA-PAH concentration obtained, for different inlet concentrations of H_2S. The individual total EPA-PAH refers to the concentration of each individual EPA-PAH, determined as the sum of each individual compound found either in the XAD-2 resin, adsorbed on soot, or on the reactor walls in each experiment tested.

Figure 2a shows that the EPA-PAH with the highest predominance are ACNY, NAPH, PHEN, FANTH, and PYR, except for ACN, FLUO, and ANTH. On the other hand, the heaviest EPA-PAH quantified from C_{18} to C_{22} were found in minor concentrations (Figure 2b). This behavior is observed for all the EPA-PAH formed in these conditions.

The concentrations of the lightest EPA-PAH (C_{10}−C_{16}) found in the pyrolysis of the C_2H_4 with different inlet concentrations of H_2S are equal to or lower than in the pyrolysis of C_2H_4 in the absence of H_2S,[18] except for NAPH and PYR (Figure 2a). In contrast, the concentrations of the heaviest EPA-PAH (C_{18}−C_{22}), which were found in the pyrolysis of C_2H_4 with 1% H_2S, are slightly higher than those found in the pyrolysis of C_2H_4 in the absence of H_2S, except for B(a)A and CHR (Figure 2b).

Additionally, the presence of 0.5% H_2S inlet concentration seems to produce a maximum in the concentration of several of the heaviest EPA-PAH such as B(a)P, I(123-cd)P, and B(ghi)P in Figure 2b, as well as PYR in Figure 2a. The predominant EPA-PAH found at 1475 K in any mixture tested is ACNY. This could be due to that NAPH is converted into ACNY, via 1-naphthylacetylene at high temperatures,[27] and it has been seen in previous works.[18,26]

Furthermore, the predominant EPA-PAH identified and quantified in each phase analyzed were similar to those found in the global quantification. Thus, the predominant EPA-PAH adsorbed on soot were ACNY, PHEN, FANTH, PYR, and B(ghi)P, in gas phase (XAD-2 resin) were NAPH and ACNY, and on the reactor walls, the highest concentration came from C_{18}−C_{22} EPA-PAH, except for CHR.

Among the different EPA-PAH, B[a]P has been identified as highly carcinogenic, and thus many guidelines, to evaluate the PAH toxicity, have been proposed by institutions, such as the World Health Organization (WHO),[28] and B[a]P has been taken as reference compound.[29] The toxicity equivalent factor (TEF)[30] is a parameter used to express the toxicity of each EPA-PAH in terms of the reference compound, B[a]P. The TEF values used in this work are shown in the Table 3. With the TEF values, it is possible to determine the benzo[a]pyrene equivalent concentration (B[a]P-eq), which is used to estimate the cancer risk attributed to the inhalation of EPA-PAH.

Table 3. Toxic Equivalence Factor (TEF) Values for Each EPA-PAH[30]

EPA-PAH	TEF value
naphthalene	0.001
acenaphthylene	0.001
acenaphthene	0.001
fluorene	0.001
phenanthrene	0.001
anthracene	0.01
fluoranthene	0.001
pyrene	0.001
benzo(a)anthracene	0.1
chrysene	0.01
benzo(b)fluoranthene	0.1
benzo(k)fluoranthene	0.1
benzo(a)pyrene	1
indeno(1,2,3-cd)pyrene	0.1
dibenz(a,h)anthracene	1
benzo(g,h,i)perylene	0.01

B[a]P-eq concentration value is the result of the sum of the different TEF values of each EPA-PAH multiplied by its measured concentration, as it is shown in eq 1, where i corresponds to each EPA-PAH measured.

$$\text{B[a]P-eq} = \sum_{i=1}^{n} (\text{TEF}_i) \times [\text{PAH}_i] \quad (1)$$

The values of B[a]P-eq and total EPA-PAH concentrations, as a function of the inlet H_2S concentration at 1475 K, are shown in Figure 3.

It is observed that the trends of the EPA-PAH concentration and the B[a]P-eq concentration are different. The EPA-PAH concentrations decrease with the amount of inlet H_2S. On the other hand, the B[a]P-eq concentration presents a maximum with the variation of inlet H_2S concentration. This indicates that the total concentration of EPA-PAH does not follow the same trend as the carcinogenic potential represented by the B[a]P-eq concentration, and both concentration of pollutants and carcinogenic potential have to be determined in order to characterize the harmful potential of an effluent.

The results shown in Figures 1−3 correspond to the maximum temperature tested in the experiments. In order to

DOI: 10.1021/acs.energyfuels.6b01271
Energy Fuels XXXX, XXX, XXX−XXX

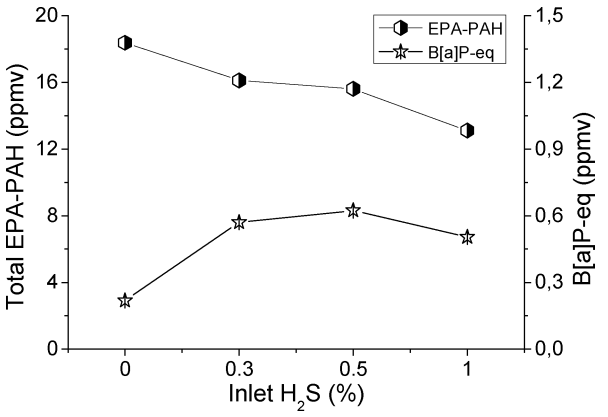

Figure 3. EPA-PAH and B[a]P-eq concentrations as a function of inlet H_2S concentration at 1475 K. Sets 1−3, 8 in Table 2.

evaluate the influence of temperature, Figure 4 shows the products obtained in the pyrolysis of a mixture of 3% C_2H_4 and 1% H_2S as a function of the reaction temperature.

The conversion of C_2H_4 increases with the temperature, and it is almost 100% above 1275 K. A similar profile is found for the conversion of H_2S, reaching conversion values of above 90% at temperatures of 1275 K and higher (Figure 4a).

Acetylene exhibits a maximum concentration at the temperature of 1175 K. The increase in C_2H_2 concentration coincides with the increase in C_2H_4 conversion indicating its origin. The decrease in C_2H_2 concentration (Figure 4a) is directly related to the temperature at which soot and EPA-PAH start to increase (Figure 4c) as a consequence of the HACA route.

The influence of temperature on C_2H_4 conversion (Figure 4a) is notable at 1175 K, when the conversion of C_2H_4 increases significantly, and the formation of CH_4 and CS_2 also increases (Figure 4b). A fraction of carbon in the reactant was taken to form these products, as it was mentioned above.

It is interesting to observe in Figure 4b the evolution of CH_4 concentration. The maximum CH_4 concentration obtained was at 1275 K. Above this temperature, CH_4 reacts very effectively with sulfur species through reactions R1−R3 producing CS_2, whose concentration is observed to increase as the temperature does.

While the soot formed progressively increases as the temperature increases (Figure 4c), the EPA-PAH and benzene amounts show a maximum at 1275 K, coinciding with the significant increase in the formation of soot. Above this temperature, benzene and EPA-PAH amounts decrease, supporting soot formation.

Furthermore, different hydrocarbons are formed during the pyrolysis of C_2H_4 in the presence of H_2S, some of them in very low concentration. Figure 5 shows the variation of these compounds concentration with temperature.

Gases such as C_2H_6, C_3H_8, and C_4H_{10} decrease their concentration as the temperature increases, and C_3H_4, C_4H_6, and C_7H_8 show a maximum at 1175 K. At higher temperatures, their concentration decreases notably.

The individual total concentration of EPA-PAH from the pyrolysis of C_2H_4 in the presence of 1% H_2S, at different reaction temperatures, from 1075 to 1475 K, is shown in Figure 6.

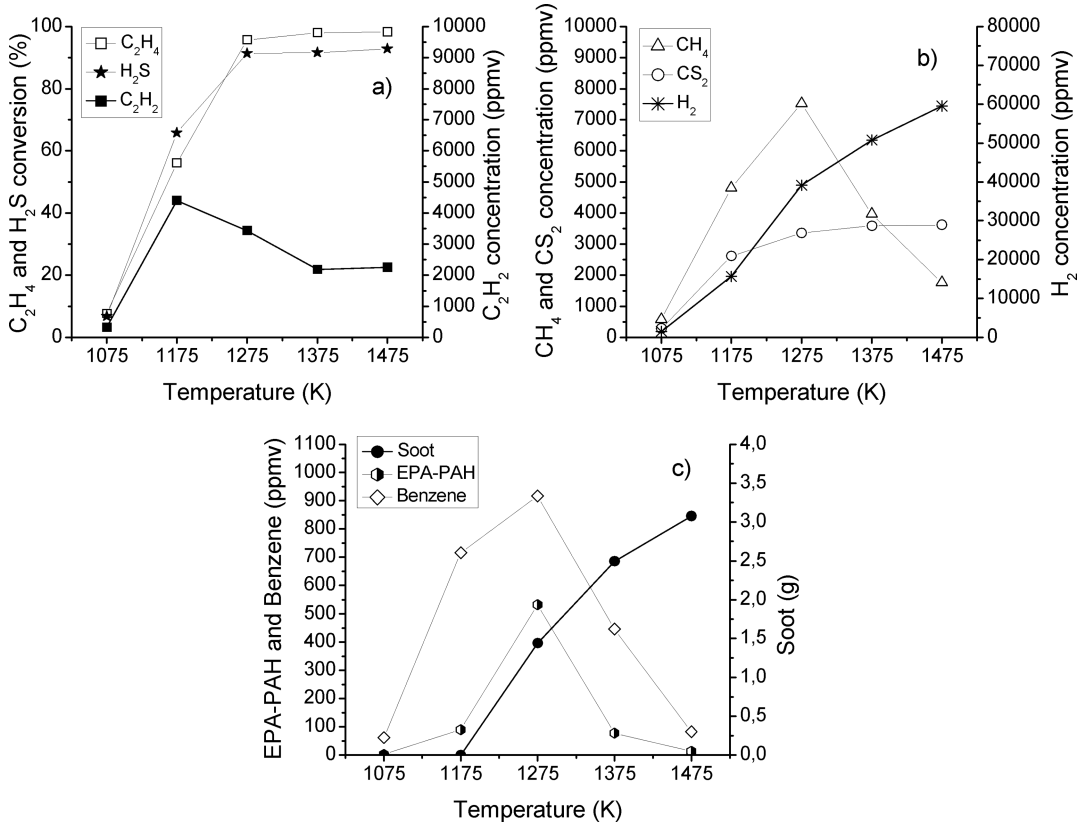

Figure 4. Products formed as a function of the temperature, $[C_2H_4]_{inlet}$: 3% and $[H_2S]_{inlet}$: 1%. (a) C_2H_4 and H_2S conversions and C_2H_2 concentration. (b) CH_4, CS_2, and H_2 concentrations. (c) Benzene, EPA-PAH, and soot amounts. Sets 3−7 in Table 2.

DOI: 10.1021/acs.energyfuels.6b01271
Energy Fuels XXXX, XXX, XXX−XXX

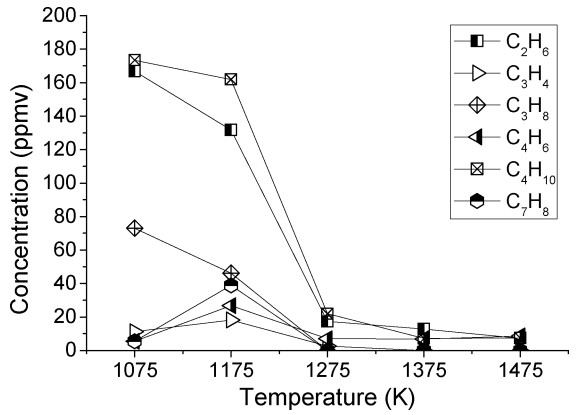

Figure 5. Hydrocarbon species concentration as a function of the temperature, $[C_2H_4]_{inlet}$: 3% and $[H_2S]_{inlet}$: 1%. Sets 3−7 in Table 2.

Figure 6a,b shows a maximum for all the EPA-PAH formed at 1275 K, which coincides with the temperature where soot begins to be significant, shown in Figure 4c. Precisely at this temperature, a higher concentration of C_{18}−C_{22} EPA-PAH is found, and this can be related to their participation, at this temperature and above, in the formation of soot.

At all temperatures tested, the amounts of NAPH and ACNY are the highest quantified, behavior already found by Sánchez et al.,[20] who related acetylene to the formation of these light EPA-PAH, via the HACA route. The C_{10}−C_{16} EPA-PAH with the highest amount were NAPH, ACNY, PHEN, FANTH, and PYR. Additionally, the EPA-PAH found in lower concentrations were from C_{18} to C_{22}.

It is worthwhile to mention that temperature has a significant influence on the distribution of EPA-PAH obtained in the different phases. For the lowest temperature studied, 1075 K, the distribution among EPA-PAH adsorbed on soot, in the outlet gas, and stuck on the reactor walls is of 13.7, 76.7 and 9.6%, respectively; and for the highest temperature tested, 1475 K, it is 67.8, 30.5, and 1.8%, respectively. This indicates that the major amount of soot formed as the temperature increases retains a higher percentage of EPA-PAH adsorbed on the soot.

The distribution of each EPA-PAH species also changes in each phase analyzed with the temperature. Thus, for example, at 1475 K, the highest concentration values were found for ACNY, PHEN, FANTH, PYR, and B(ghi)P on soot, NAPH and ACNY in gas phase, and C_{18}−C_{22}, except for CHR, on the reactor walls. At low temperatures such as 1175 K, the highest values were found for NAPH, ACNY, FLUO, FANTH, and PYR on soot, NAPH in gas phase, and NAPH, ACNY, PHEN, ANTH, FANTH, and PYR on the reactor walls.

On the other hand, Figure 7 shows the values of B[a]P-eq and total EPA-PAH concentrations as a function of the reaction temperature.

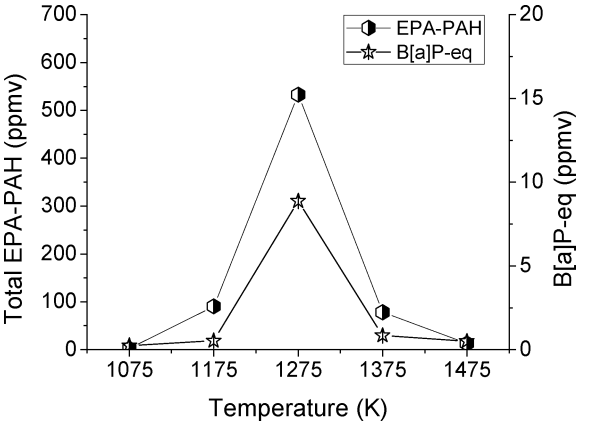

Figure 7. EPA-PAH and B[a]P-eq concentrations as a function of the temperature, $[C_2H_4]_{inlet}$: 3% and $[H_2S]_{inlet}$: 1%. Sets 3−7 in Table 2.

In comparison to the analysis of the influence of the inlet H_2S concentration, in this case, the trends of the variation of B[a]P-eq and total EPA-PAH concentrations are similar and show a maximum at 1275 K. This tendency could be explained by the significant formation of soot at this temperature shown in Figure 4c.

4. CONCLUSIONS

The present work shows the influence of the H_2S presence on the pyrolysis of ethylene and analyzes its impact over the light gases, EPA-PAH, and soot formed. Experiments were performed with a given inlet ethylene concentration, 3% by volume, and with different inlet H_2S concentrations, specifically 0, 0.3, 0.5 and 1% by volume. The temperature ranged from 1075 to 1475 K. The main conclusions are the following.

There is an effective interaction between H_2S and hydrocarbons, such as C_2H_4 and CH_4, during the pyrolysis of C_2H_4−H_2S mixtures, deduced by the formation of significant amounts

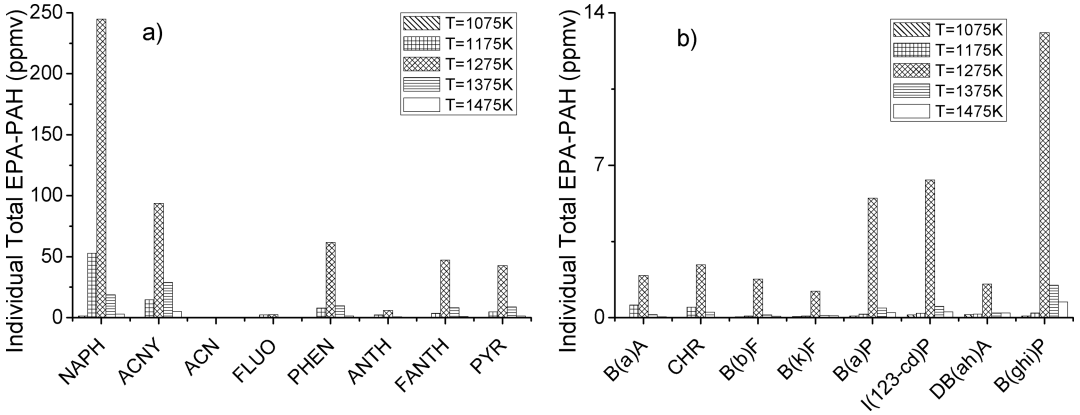

Figure 6. Individual total EPA-PAH concentration as a function of the reaction temperature, [C_2H_4]inlet: 3% and [H_2S]inlet: 1%. (a) EPA-PAH (C_{10}−C_{16}). (b) EPA-PAH (C_{18}−C_{22}). Sets 3−7 in Table 2.

DOI: 10.1021/acs.energyfuels.6b01271
Energy Fuels XXXX, XXX, XXX−XXX

of CS_2 and the presence of sulfur in the elemental analysis of soot formed.

The presence of H_2S acts to slightly decrease the formation of soot and EPA-PAH, which indicates a positive effect of this sulfur compound under pyrolysis conditions, despite its reducing character.

The total EPA-PAH and B[a]P-eq concentrations follow different trends as the H_2S inlet concentration increases, but similar trends regarding the influence of the temperature. Thus, the determination of the concentration of EPA-PAH and B[a]P-eq must be done separately, which could be useful to evaluate the harmful potential of an effluent.

The effect of the temperature is important, increasing the formation of CS_2 from 1175 K, and also affecting the formation of EPA-PAH, showing a maximum at 1275 K, which coincides with the significant formation of soot.

The EPA-PAH found in the highest amounts were NAPH, ACNY, PHEN, FANTH, and PYR, whereas the EPA-PAH found in the lowest amounts were ACN, FLUO, ANTH, B(a)A, CHR, B(b)F, B(k)F, B(a)P, I(123-cd)P, DB(ah)A, and B(ghi)P. The predominance of two EPA-PAH, NAPH and ACNY, was observed for all the cases studied.

AUTHOR INFORMATION

Corresponding Author

*E-mail: uxue@unizar.es.

Notes

The authors declare no competing financial interest.

ACKNOWLEDGMENTS

The authors express their gratitude to Aragon Government and European Social Fund (GPT group), and MINECO and FEDER (Project CTQ2015-65226), for financial support. F.V. acknowledges the "Secretaría Nacional de Educación Superior, Ciencia, Tecnología e Innovación" (SENESCYT) of Ecuador, for the predoctoral grant awarded.

REFERENCES

(1) Rojey, A.; Jaffret, C.; Cornot-Gandolphe, S.; Durand, B.; Jullian, S.; Valais, M. *Natural Gas: Production Processing Transport*; Technip: Paris, France, 1997; p 429.

(2) Burgers, W. F. J.; Northrop, P. S.; Kheshgi, H. S.; Valencia, J. A. *Energy Procedia* **2011**, *4*, 2178−2184.

(3) Bongartz, D.; Ghoniem, A. F. *Combust. Flame* **2015**, *162*, 544−553.

(4) Mora, R. L. *J. Hazard. Mater.* **2000**, *79*, 103−115.

(5) Mohammed, S.; Raj, A.; Al Shoaibi, A.; Sivashanmugam, P. *Chem. Eng. Sci.* **2015**, *137*, 91−105.

(6) Wang, H.; Frenklach, M. *Combust. Flame* **1997**, *110*, 173−221.

(7) Agency for Toxic Substances and Disease Registry (ATSDR). *Toxicological Profile for Polycyclic Aromatic Hydrocarbons*; 1995. ATSDR Web Site. http://www.atsdr.cdc.gov/toxprofiles/tp69.pdf (accessed May 18, 2016).

(8) Selim, H.; Al Shoaibi, A.; Gupta, A. K. *Appl. Energy* **2012**, *92*, 57−64.

(9) Chin, H. S. F.; Karan, K.; Mehrotra, A. K.; Behie, L. A. *Can. J. Chem. Eng.* **2001**, *79*, 482−490.

(10) Glarborg, P.; Marshall, P. *Int. J. Chem. Kinet.* **2013**, *45*, 429−439.

(11) Glarborg, P.; Halaburt, B.; Marshall, P.; Guillory, A.; Troe, J.; Thellefsen, M.; Christensen, K. *J. Phys. Chem. A* **2014**, *118*, 6798−6809.

(12) Abián, M.; Cebrián, M.; Millera, Á.; Bilbao, R.; Alzueta, M. U. *Combust. Flame* **2015**, *162*, 2119−2127.

(13) Bongartz, D.; Ghoniem, A. F. *Combust. Flame* **2015**, *162*, 2749−2757.

(14) Lawton, S. A. *Combust. Flame* **1989**, *75*, 175−181.

(15) Gülder, Ö.L. *Combust. Flame* **1993**, *92*, 410−418.

(16) Abián, M.; Millera, Á.; Bilbao, R.; Alzueta, M. U. *Fuel* **2015**, *159*, 550−558.

(17) Streibel, T.; Mühlberger, F.; Geißler, R.; Saraji-Bozorgzad, M.; Adam, T.; Zimmermann, R. *Proc. Combust. Inst.* **2015**, *35*, 1771−1777.

(18) Viteri, F.; Abián, M.; Millera, Á.; Bilbao, R.; Alzueta, M. U. *Fuel* **2016**, *184*, 966−972.

(19) U.S. Environmental Protection Agency (EPA). *Health Assessment Document For Diesel Engine Exhaust*; 2002. EPA Web site. http://hero.epa.gov/index.cfm/reference/download/reference_id/42866 (accessed May 18, 2016).

(20) Sánchez, N. E.; Millera, Á.; Bilbao, R.; Alzueta, M. U. *J. Anal. Appl. Pyrolysis* **2013**, *103*, 126−133.

(21) Sánchez, N. E.; Callejas, A.; Millera, Á.; Bilbao, R.; Alzueta, M. U. *Energy Fuels* **2013**, *27*, 7081−7088.

(22) Sánchez, N. E.; Callejas, A.; Millera, Á.; Bilbao, R.; Alzueta, M. U. *Energy* **2012**, *43*, 30−36.

(23) Sánchez, N. E.; Salafranca, J.; Callejas, A.; Millera, Á.; Bilbao, R.; Alzueta, M. U. *Fuel* **2013**, *107*, 246−253.

(24) U.S. Environmental Protection Agency (EPA). *Compendium of Methods for the Determination of Toxic Organic Compounds in Ambient Air*; Method TO-13A; 1999. EPA Web site. https://www3.epa.gov/ttnamti1/files/ambient/airtox/to-13arr.pdf (accessed May 18, 2016).

(25) Karan, K.; Behie, L. A. *Ind. Eng. Chem. Res.* **2004**, *43*, 3304−3313.

(26) Sánchez, N. E.; Callejas, A.; Millera, Á.; Bilbao, R.; Alzueta, M. U. *Energy Fuels* **2012**, *26*, 4823−4829.

(27) Richter, H.; Mazyar, O. A.; Sumathi, R.; Green, W. H.; Howard, J. B.; Bozzelli, J. W. *J. Phys. Chem. A* **2001**, *105*, 1561−1573.

(28) World Health Organization WHO. *Air Quality Guidelines for Europe*; 2000. WHO Regional Office for Europe Web site. http://www.euro.who.int/__data/assets/pdf_file/0005/74732/E71922.pdf (accessed May 18, 2016).

(29) Jia, Y.; Stone, D.; Wang, W.; Schrlau, J.; Tao, S.; Simonich, S. L. M. *Environ. Health Perspect.* **2011**, *119*, 815−820.

(30) Nisbet, I. C. T.; LaGoy, P. K. *Regul. Toxicol. Pharmacol.* **1992**, *16*, 290−300.

DOI: 10.1021/acs.energyfuels.6b01271
Energy Fuels XXXX, XXX, XXX−XXX